



Peritumoral-to-tumoral apparent diffusion coefficient ratio as a marker of tumor microenvironment activity across breast cancer molecular subtypes

Seçil Gündoğdu¹
 Eda Elverici¹
 Arzu Özsoy²
 Leman Günbey Karabekmez³
 Muhammed Said Beşler⁴
 Emre Gündoğdu⁵

¹Ankara Bilkent City Hospital, Clinic of Radiology, Ankara, Türkiye

²Ankara Medipol University Faculty of Medicine, Department of Radiology, Ankara, Türkiye

³Ankara Bilkent City Hospital, Yıldırım Beyazıt University, Department of Radiology, Ankara, Türkiye

⁴İstanbul Medeniyet University Faculty of Medicine, Department of Radiology, İstanbul, Türkiye

⁵Yüksek İhtisas University Faculty of Medicine, Department of Surgery, Ankara, Türkiye

Corresponding author: Seçil Gündoğdu

E-mail: drsecilgundogdu@gmail.com

Received 11 November 2025; revision requested 26 December 2025; accepted 11 February 2026.



Epub: 26.02.2026

Publication date:

DOI: 10.4274/dir.2026.263742

PURPOSE

This study aimed to evaluate the prognostic significance of tumoral apparent diffusion coefficient (tADC), peritumoral ADC (pADC), and the peritumoral-to-tumoral ADC (p/tADC) ratio in invasive breast cancers using high-resolution diffusion-weighted imaging.

METHODS

A retrospective cohort of 149 patients with invasive breast cancer was analyzed. pADC, tADC, and p/tADC values were independently measured by two experienced radiologists. The associations between these parameters and histological grade, receptor status, Ki-67 index, and molecular subtypes were assessed. Interobserver agreement was evaluated using the intraclass correlation coefficient (ICC), and multivariate logistic regression was performed to identify independent predictors.

RESULTS

Although tADC was significantly associated only with tumor size ($P < 0.050$), both pADC and p/tADC were significantly associated with high histological grade, estrogen receptor/progesterone receptor negativity, human epidermal growth factor receptor 2 positivity, and high Ki-67 index ($P < 0.01$). The p/tADC ratio emerged as an independent predictor of high-grade tumors and Ki-67 $\geq 20\%$. Excellent interobserver agreement was observed for all ADC measurements (ICC > 0.90).

CONCLUSION

The p/tADC ratio reflects stromal and microenvironmental alterations associated with tumor aggressiveness and demonstrates stronger prognostic relevance than tADC alone. Incorporating the p/tADC ratio into routine magnetic resonance imaging (MRI) interpretation may improve preoperative risk stratification and support personalized treatment planning in invasive breast cancer.

CLINICAL SIGNIFICANCE

The p/tADC ratio reflects stromal and microenvironmental changes associated with tumor aggressiveness and may serve as a noninvasive imaging biomarker. Its integration into preoperative MRI protocols may facilitate risk stratification and personalized treatment planning.

KEYWORDS

Breast cancer, diffusion-weighted magnetic resonance imaging, apparent diffusion coefficient, tumor microenvironment, molecular subtype, Ki-67, human epidermal growth factor receptor 2, peritumoral region, prognostic imaging biomarker

Breast cancer is among the most frequently encountered malignancies worldwide, with an annual incidence of approximately 2.3 million cases and over 666,000 deaths, ranking as the fourth leading cause of cancer-related mortality.¹ To address this burden, global efforts have intensified through early detection strategies, including national screening programs and awareness campaigns.

Tumor microenvironment

Breast cancers exhibit remarkable heterogeneity in both genetic and cellular behavior, influencing disease progression and treatment response.^{2,3} The tumor microenvironment (TME)—comprising immune cells, fibroblasts, and the extracellular matrix—plays a pivotal role in tumor development.⁴⁻⁹ In invasive breast cancers, phenomena such as lymphatic obstruction and matrix remodeling around tumors contribute to peritumoral edema, a known feature of malignancy.⁵ This edema, linked to increased vascular permeability via proteolytic enzymes and angiogenesis, has been associated with more aggressive tumor behavior and poorer prognosis.¹⁰⁻¹³ Notably, the peritumoral stroma harbors genetic distinctions from intratumoral regions, suggesting it provides biologically distinct and prognostically relevant information.¹⁴⁻¹⁶

Magnetic resonance imaging and diffusion-weighted imaging

Magnetic resonance imaging (MRI) offers superior sensitivity for breast cancer detection, enabling detailed anatomical and functional assessments.¹⁷ However, its specificity remains limited.¹⁸ Diffusion-weighted imaging (DWI), which measures water-molecule movement, enhances diagnostic accuracy by providing apparent diffusion coefficient (ADC) values, which are typically lower in malignant tissues due to higher cellularity.¹⁹⁻²²

Several studies have explored correlations between ADC values and histopathologic features, including tumor size, grade, lymphovascular invasion, nodal status, and molecular subtype; however, results have been inconsistent due to methodological variability.²³⁻²⁵ Peritumoral edema has emerged as a promising imaging marker, but limited data exist on its association with histopathologic aggressiveness or DWI parameters.^{26,27}

In this study, the term peritumoral region specifically refers to the stromal tissue sur-

rounding the tumor rather than to peritumoral edema alone. Although peritumoral edema seen on T2-weighted imaging may be a visual manifestation of stromal changes, our diffusion-weighted analysis focused on quantitative ADC measurements from the biologically active peritumoral stroma, excluding cystic, necrotic, or purely edematous regions.

Aim

This study investigates the relationship between MRI features and histopathological characteristics of breast cancer, with a specific focus on the prognostic significance of the peritumoral-to-tumoral ADC (p/tADC) ratio.

Methods

Study group

This retrospective study was conducted with the approval of the Ethics Committee of Ankara Bilkent City Hospital (decision number: E1-23-3199, date: 11.01.2023). Between April 2020 and July 2023, 367 patients who underwent high-resolution DWI with a narrow-field-of-view protocol on a 3-Tesla (T) MRI scanner were reviewed. Among these, 149 women (mean age: 53 ± 10.5 years; range 33–86 years) who had preoperative breast MRI- and biopsy-confirmed invasive breast cancer were included in the study. Patients with pure in situ carcinoma, a prior history of neoadjuvant chemotherapy, or the absence of surgery following breast MRI were excluded from the study.

Demographic data and the pathology reports of the patients were retrieved from the hospital information management system.

The patient selection process is summarized in Figure 1.

Magnetic resonance imaging protocol

All breast MRI examinations were performed on a 3.0-T scanner (Signa Pioneer, General Electric Medical Systems, Milwaukee, WI, USA) in the prone position using a dedicated 16-channel phased-array bilateral breast coil (NeoCoil 3.0 T, General Electric Medical Systems, Milwaukee, WI, USA).

The imaging protocol included the following sequences:

- Axial T1-weighted fast spin-echo [repetition time (TR)/echo time (TE): 484/8.5 ms; slice thickness: 5 mm]
- Axial and sagittal T2-weighted fat-suppressed fast spin-echo (TR/TE: 4,786/82.5 ms

and 5,116/83.5 ms, respectively; slice thickness: 5 mm)

- Dynamic contrast-enhanced (DCE) axial T1-weighted fat-suppressed sequence (TR/TE: 6.1/1.7 ms; slice thickness: 2.2 mm), acquired before and after intravenous administration of a gadolinium-based contrast agent (0.1 mmol/kg), followed by a 20-mL saline flush

- DWI using single-shot echo-planar imaging with b values of 50 and 800 s/mm². ADC maps were automatically generated on the workstation.

Histopathological evaluation

Histopathological specimens obtained from surgical samples were evaluated by the Pathology Department of Ankara Bilkent City Hospital. Pathological data included information on estrogen receptor (ER) status, progesterone receptor (PR) status, human epidermal growth factor receptor 2 (HER2) status, Ki-67 index, and tumor size.

Apparent diffusion coefficient measurements

ADC measurements and T1-weighted, T2-weighted, and DCE images were used for anatomical reference. On the ADC map, the slice with the largest lesion cross-sectional diameter was selected. For tADC measurement, a circular region of interest (ROI) with a fixed diameter of 10 pixels (approximately 10 mm²) was manually placed within the most restricted (visually darkest) solid portion of the tumor, avoiding necrotic, cystic, hemorrhagic, and fatty areas. The lowest ADC value obtained from three measurements was recorded as the representative tADC. For peritumoral ADC (pADC) assessment, three ROIs of identical size and shape (10 pixels in diameter) were placed in the adjacent breast parenchyma within a 5–10 mm distance from the tumor border, excluding fibroglandular tissue, large vessels, ducts, and artifacts. These ROIs were placed in areas with the highest signal intensity on the ADC map, consistent with increased diffusivity. Among these, the highest ADC value was recorded as the pADC, in line with previously published methods.²⁸ The p/tADC ratio was calculated by dividing the pADC by the tADC. Sample images of tumors with high and low pADC values were shown in Figures 2 and 3, respectively. All measurements were performed by two radiologists with over 5 years of experience in breast imaging. Each measurement was performed independently, and the mean value was used for analysis. The interobserv-

Main points

- The peritumoral-to-tumoral apparent diffusion coefficient (p/tADC) ratio is significantly elevated in tumors with aggressive biological features.
- Unlike tumoral ADC, peritumoral ADC and p/tADC show robust correlations with multiple prognostic markers.
- ADC measurements demonstrated excellent interobserver reproducibility, supporting their clinical reliability.

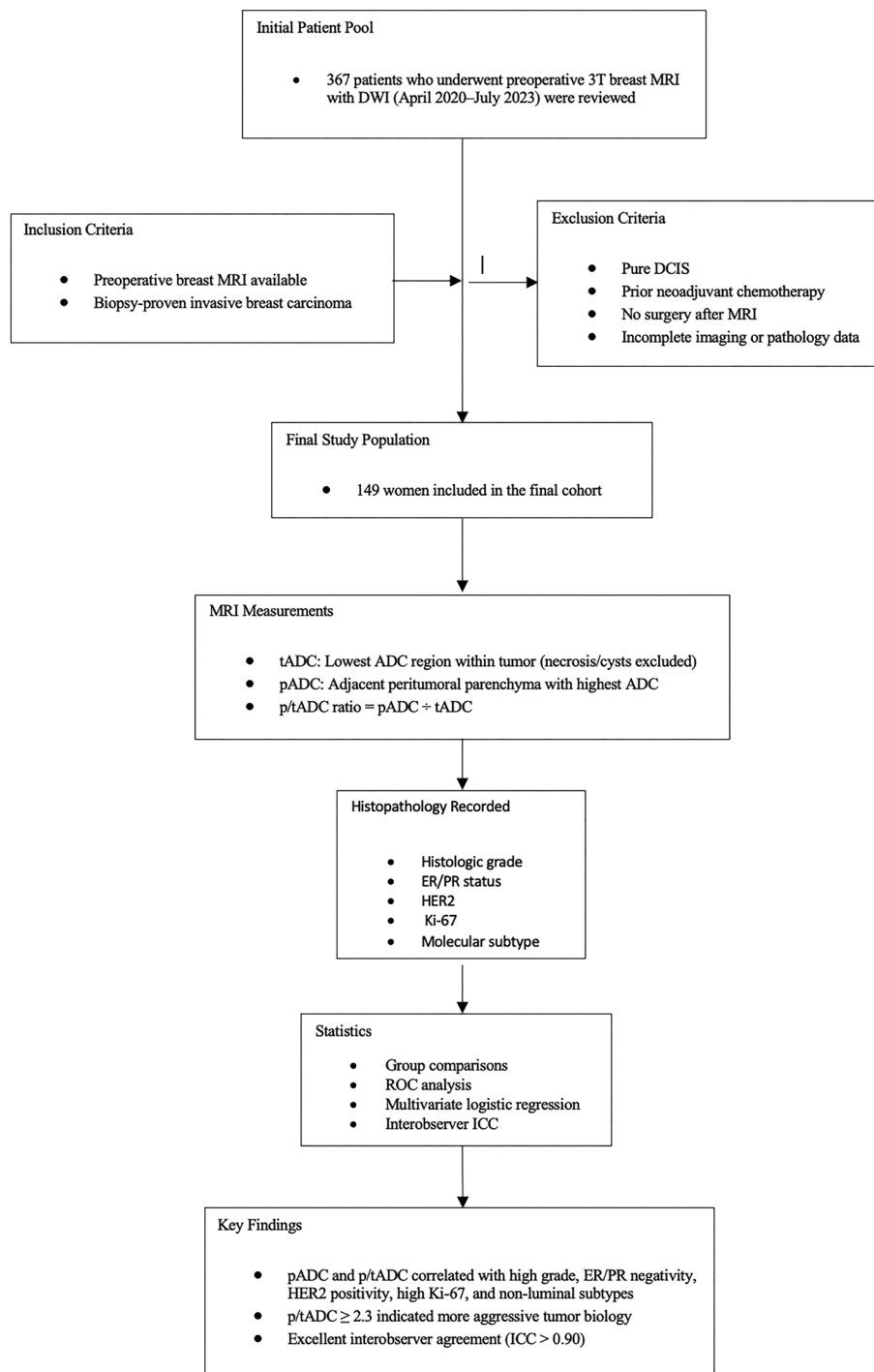


Figure 1. Flow diagram of the patient selection process. MRI, magnetic resonance imaging; DWI, diffusion-weighted imaging; DCIS, ductal carcinoma *in situ*; ADC, apparent diffusion coefficient; p/tADC, peritumoral-to-tumoral apparent diffusion coefficient; pADC, peritumoral apparent diffusion coefficient value; tADC, tumoral apparent diffusion coefficient value; ER, estrogen receptor; PR, progesterone receptor; HER2, human epidermal growth factor 2; ROC, receiver operating characteristic; ICC, intraclass correlation coefficient.

er agreement was assessed using the intraclass correlation coefficient (ICC).

Pathological assessment

All patients underwent pathological evaluation of surgical specimens. Parameters such as histological grade, ER status, PR

status, HER2 status, Ki-67 index, and axillary lymph node status were analyzed as binary variables as follows:

- ER/PR status was evaluated using the Allred scoring system, and a total score >2 was considered positive.

- The HER2 score was evaluated immunohistochemically on a scale of 0–3; scores of 0–1 were considered negative, and a score of 3 was considered positive. Cases with a score of 2 underwent further evaluation with fluorescent *in situ* hybridization testing.

- Ki-67 values < 20% were classified as negative and values ≥ 20% as positive.

Statistical analysis

All statistical analyses were performed using SPSS version 30.0 (IBM, Chicago, IL, USA). ADC values were considered continuous dependent variables. Histopathological parameters were treated as binary independent variables, including the following:

- Histological grade: Grade 1–2 vs. Grade 3
- ER and PR status: Negative vs. Positive
- HER2 status: Negative vs. Positive
- Ki-67: < 20% vs. ≥ 20%
- Axillary lymph node metastasis: Negative vs. Positive
- Tumor type: Ductal vs. Lobular
- Molecular subtype: Luminal (luminal A, luminal B and luminal B-HER2+) vs. non-luminal (HER2-enriched, basal-like)

The normality of data distribution was assessed using the Shapiro–Wilk test. For normally distributed variables, comparisons between two groups were conducted using the independent samples Student’s t-test, and results were expressed as mean ± standard deviation (SD).

For comparisons among luminal molecular subtypes (luminal A, luminal B, luminal B-HER2+, HER2-enriched, and basal-like), one-way analysis of variance was performed. When overall significance was observed, post-hoc pairwise comparisons were conducted using the Tukey test to identify intergroup differences.

Two-tailed tests were used for all analyses, and a *P* value < 0.05 was considered statistically significant.

Receiver operating characteristic (ROC) curve analysis was performed to determine optimal cut-off values for the p/tADC ratio to predict aggressive tumor characteristics. For each cut-off, sensitivity, specificity, and positive likelihood ratios (LR+) were calculated to assess discriminative performance.

Variables with $P < 0.05$ in univariate analysis were entered into a multivariate binary logistic regression model to identify independent predictors of a high p/tADC ratio. The p/tADC ratio was dichotomized at 2.3 based on ROC analysis; ROC curves were generated to evaluate the ability of the p/tADC ratio to distinguish high-grade tumors (grade 3) and a high Ki-67 index ($\geq 20\%$) from lower-risk tumors. The cut-off value was selected by maximizing the Youden index across these prognostic measures. Model calibration and performance were assessed using the Hosmer–Lemeshow goodness-of-fit test and Nagelkerke R^2 .

Interobserver agreement

To assess measurement reproducibility between the two radiologists, interobserver agreement was evaluated for tADC, pADC, and p/tADC values in a randomly selected subset of 40 lesions (approximately 25% of the sample). The ICC (two-way random-effects model, absolute agreement) was calculated. Agreement was interpreted as follows: poor (< 0.50), moderate (0.50–0.75), good (0.75–0.90), and excellent (> 0.90).

Additionally, Bland–Altman plots were generated to visualize systematic bias and 95% limits of agreement between the two observers for each parameter.

Results

Between April 2020 and July 2023, a total of 149 women (mean age: 53 ± 10.5 years; range: 33–86 years) with invasive breast cancer were included in the study.

Interobserver agreement

Excellent interobserver agreement was observed for all ADC-based measurements. The ICC values for tADC, pADC, and the p/tADC ratio were 0.94 [95% confidence interval (CI): 0.90–0.97], 0.91 (95% CI: 0.86–0.95), and 0.93 (95% CI: 0.88–0.96), respectively (all $P < 0.001$).

Bland–Altman analysis demonstrated a mean difference of $0.02 \times 10^{-3} \text{ mm}^2/\text{s}$ for tADC and $0.05 \times 10^{-3} \text{ mm}^2/\text{s}$ for pADC, with no significant proportional bias. All differences lay within ± 1.96 SD, confirming acceptable agreement between readers (Table 1).

Demographic data and tumor characteristics are summarized in Table 2.

tADC values were significantly associated with tumor size ($P = 0.005$). However, no significant associations were found with

histological grade ($P = 0.252$), Ki-67 index ($P = 0.635$), ER ($P = 0.562$), PR ($P = 0.652$), HER2 ($P = 0.556$), axillary lymph node status ($P = 0.957$), or molecular subtype ($P = 0.703$).

pADC was significantly associated with tumor size ($P = 0.009$), axillary lymph node positivity ($P = 0.02$), molecular subtype ($P < 0.001$), HER2 ($P = 0.002$), ER ($P = 0.001$),

PR ($P = 0.002$), Ki-67 ($P < 0.001$), and histological grade ($P = 0.010$).

The p/tADC ratio showed significant associations with tumor size ($P < 0.001$), histological grade ($P = 0.004$), Ki-67 index ($P < 0.001$), ER ($P = 0.006$), PR ($P = 0.015$), and HER2 ($P = 0.010$) but not with lymph node positivity ($P = 0.08$).

Table 1. Bland–Altman plots illustrating interobserver agreement for tADC, pADC, and p/tADC measurements

Parameter	ICC (95% CI)	<i>P</i> value	Interpretation
tADC	0.94 (0.90–0.97)	<0.001	Excellent
pADC	0.91 (0.86–0.95)	<0.001	Excellent
p/tADC	0.93 (0.88–0.96)	<0.001	Excellent

tADC, tumoral apparent diffusion coefficient; pADC, peritumoral apparent diffusion coefficient; p/tADC, peritumoral-to-tumoral apparent diffusion coefficient; ICC, intraclass correlation coefficient; CI, confidence interval.

Table 2. Patients' demographic data and tumor characteristics

Number of patients	149
Age (years) (mean \pm SD)	53 ± 10.5
Tumor size (mean \pm SD)	3.01 ± 1.77
Lymph node	
Positive	67 (45%)
Negative	82 (55%)
Grade	
G1	28 (18.8%)
G2	92 (61.7%)
G3	29 (19.5%)
Estrogen receptor	
Positive	117 (78.5%)
Negative	32 (21.5%)
Progesterone receptor	
Positive	115 (77.2%)
Negative	34 (22.8%)
HER2 receptor	
Positive	106 (71.1%)
Negative	43 (28.9%)
Ki-67 expression	
< 20%	59 (39.6%)
$\geq 20\%$	90 (60.4%)
Tumor type	
Ductal	132 (88.6%)
Lobular	14 (9.4%)
Others	3 (2%)
Luminal subtype	
Luminal A	52 (34.9%)
Luminal B	37 (24.8%)
Luminal B/HER2 +	30 (20.1%)
HER2 overexpression	12 (8.1%)
Basal-Like	18 (12.1%)

SD, standard deviation; HER2, human epidermal growth factor 2.

Associations between pADC and tADC values, p/tADC ratios, histopathological parameters, and lymph nodes status are shown in Table 3.

Comparison by molecular subtype

No statistically significant difference in tADC values was observed between luminal and non-luminal subgroups ($P = 0.703$). By contrast, both pADC and p/tADC values demonstrated a statistically significant difference among the luminal subtypes ($P < 0.001$ and $P = 0.002$, respectively).

No statistically significant differences in pADC ($P = 0.085$) or p/tADC ratios ($P = 0.327$) were observed between luminal A and luminal B groups. However, the luminal A group demonstrated significantly lower pADC and p/tADC ratios than the luminal B-HER2+ ($P = 0.003$, $P = 0.007$, respectively), HER2-enriched ($P < 0.001$, $P = 0.035$, respectively), and basal-like tumor groups ($P = 0.001$, $P = 0.003$, respectively).

By contrast, no significant differences were found among the luminal B, luminal B-HER2+, HER2-enriched, and basal-like groups in terms of pADC and p/tADC ratios. Additionally, tADC values did not differ significantly across molecular subtypes.

Prognostic performance of peritumoral-to-tumoral apparent diffusion coefficient ratios

Analysis of the prognostic predictive power of the p/tADC ratio revealed the highest discriminative performance for tumor

size (LR+: 1.99), whereas the lowest was observed for HER2 status (LR+: 1.56). Cut-off values, sensitivity, specificity, and LR+ are summarized in Table 4.

Multivariate logistic regression

In the multivariate logistic regression analysis, the model demonstrated acceptable fit (Hosmer–Lemeshow χ^2 : 11.55, df: 8, $P = 0.17$) and accounted for approximately 24% of the variance in the high p/tADC ratio (Nagelkerke R^2 : 0.24). High histological grade and a Ki-67 index $\geq 20\%$ were identified as independent predictors of a high p/tADC ratio (≥ 2.3), whereas ER, PR, and HER2 status did not remain significant in the multivariate model (Table 5). The ROC analysis confirmed that a p/tADC threshold of 2.3 provided the optimal balance of sensitivity and specificity for differentiating high-grade tumors and elevated Ki-67 expression.

Discussion

This study underscores the prognostic potential of the p/tADC ratio as a non-invasive imaging biomarker in invasive breast cancer. We demonstrated that although tADC was significantly associated only with tumor size, the p/tADC ratio showed independent associations with high histological grade and elevated Ki-67 index and was significantly different across molecular subtypes. These findings suggest that alterations in diffusion within the peritumoral microenvironment provide clinically relevant biological information beyond what tADC alone can reveal.

The inverse association between ADC values and cellularity is well established, as lower tADC values often indicate high cellular density and reduced extracellular space.^{23,29} However, prior studies have reported inconsistent correlations between ADC and key pathological markers such as receptor status, Ki-67, and tumor grade.^{20,30} Our findings are consistent with this inconsistency, as tADC did not correlate significantly with ER, PR, HER2, or Ki-67 in our cohort.

Interobserver agreement for all diffusion metrics was excellent (ICC > 0.90), confirming the reproducibility of our measurement protocol.

In contrast to tADC, both pADC and the p/tADC ratio showed significant associations with histological grade, hormone receptor status, HER2 expression, and Ki-67 index. This supports the notion that the peritumoral stroma is an active component of the TME and may mirror stromal remodeling, angiogenesis, immune suppression, and extracellular matrix changes.^{6,16,31,32}

Several histopathological and imaging-based studies have identified edema, inflammation, and stromal activation in peritumoral tissues of high-grade tumors.^{11,33} Zhang et al.³³ showed that peritumoral edema is more pronounced in HER2+ and triple-negative tumors, reflecting elevated vascular permeability and cytokine-mediated stromal stress.³⁴ These findings are further supported by DWI-based studies linking high pADC values to HER2 overexpression and high Ki-67,^{12,35} which align with our ob-

Table 3. Associations between tumor and peritumor ADC values, p/tADC ratios, histopathological parameters, and lymph node status

	Tumor size	LN	Histologic subtype	HER2	ER	PR	Ki67	Grade
p/tADC	< 0.001	0.08	0.002	0.010	0.006	0.015	< 0.001	0.004
pADC	0.009	0.02	0.001	0.002	0.001	0.002	< 0.001	0.010
tADC	0.005	0.957	0.703	0.556	0.562	0.652	0.635	0.252

ADC, apparent diffusion coefficient; p/tADC, peritumoral-to-tumoral apparent diffusion coefficient; pADC, peritumoral apparent diffusion coefficient value; tADC, tumoral apparent diffusion coefficient value; LN, lymph node metastasis; HER2, human epidermal growth factor 2; ER, estrogen receptor, PR, progesterone receptor.

Table 4. Cut-off values, sensitivity, specificity, and positive likelihood ratios of p/tADC ratios

ADC ratio	Cut-off value	Sensitivity (%)	Specificity (%)	LR+	P value
Tumor size > 2cm	2.3	66.3	66.7	1.99	0.00
Grade	2.6313	65.5	65.8	1.92	0.002
Molecular subtype	2.5496	63.3	62.2	1.67	0.00
ER negativity	2.5496	62.5	62.4	1.66	0.002
PR negativity	2.537	61.8	60.9	1.58	0.005
HER2	2.5162	60.5	61.3	1.56	0.006
Ki-67	2.3581	61.1	61	1.57	0.00

ADC, apparent diffusion coefficient; p/tADC, peritumoral-to-tumoral apparent diffusion coefficient; ER, estrogen receptor; PR, progesterone receptor; HER2, human epidermal growth factor 2; LR+, positive likelihood ratio.

Table 5. Multivariate logistic regression analysis identifying independent predictors of high p/tADC ratio.

Variable	Univariate p	Multivariate OR (95% CI)	P value
ER negative	0.006	1.8 (0.9–3.6)	0.09
PR negative	0.015	1.5 (0.7–3.0)	0.18
HER2 positive	0.010	1.7 (0.8–3.2)	0.11
Ki-67 $\geq 20\%$	<0.001	2.9 (1.5–5.8)	0.002
Grade 3	0.004	2.3 (1.1–4.7)	0.021

OR, odds ratio; CI, confidence interval; ER, estrogen receptor; PR, progesterone receptor; HER2, human epidermal growth factor 2.

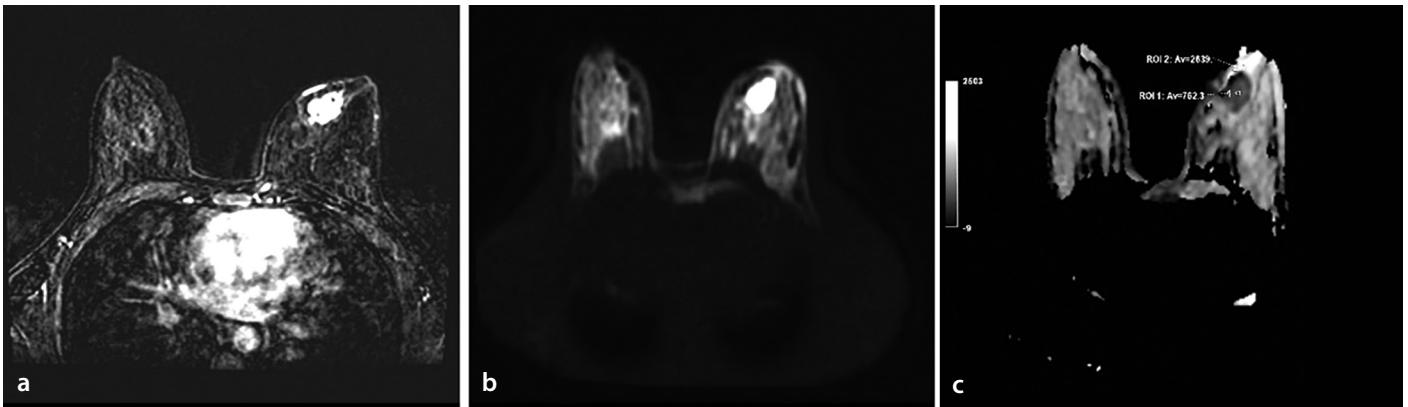


Figure 2. Breast lesion in a 52-year-old female patient with a high peritumor/tumor apparent diffusion coefficient (ADC) ratio. (a) Axial T1-weighted fat-suppressed dynamic sequence shows a mass with heterogeneous enhancement in the left breast; (b) high peritumoral signal intensity is shown in Axial T2-weighted fat-suppressed sequence; (c) the ADC map shows restricted diffusion in the mass. The lowest mean tumor ADC value (shown as ROI_{tumor}) was $0.7 \times 10^{-3} \text{ mm}^2/\text{s}$, and the highest mean peritumor ADC value (shown as ROI_{peritumor}) was $2.6 \times 10^{-3} \text{ mm}^2/\text{s}$. The peritumor/tumor ADC ratio was 3.71. The clinical and histopathological features of the lesion were grade 3, human epidermal growth factor receptor 2 positive, estrogen receptor and progesterone receptor negative, Ki-67 high ($> 20\%$).

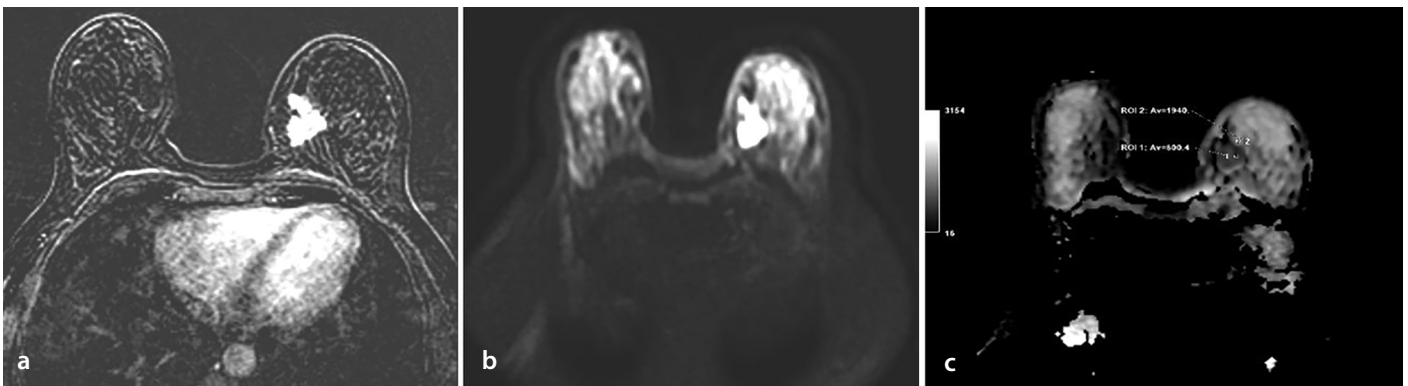


Figure 3. Breast lesion in a 63-year-old female patient with a low peritumor/tumor apparent diffusion coefficient (ADC) ratio. (a) Axial T1-weighted fat-suppressed dynamic sequence shows a mass with irregular margin and heterogeneous enhancement in the left breast; (b) normal peritumoral signal intensity is shown in axial T2-weighted fat-suppressed sequence; (c) the ADC map shows restricted diffusion in the mass. The lowest mean tumor ADC value (shown as ROI_{tumor}) was $0.8 \times 10^{-3} \text{ mm}^2/\text{s}$, and the highest mean peritumor ADC value (shown as ROI_{peritumor}) was $1.9 \times 10^{-3} \text{ mm}^2/\text{s}$. The peritumor/tumor ADC ratio was 2.3. The clinical and histopathological features of the lesion were: grade 1, estrogen receptor and progesterone receptor negative, Ki-67 low ($< 20\%$).

servation that aggressive tumors exhibit higher pADC and p/tADC ratios.

From a molecular perspective, our analysis revealed that HER2-enriched, basal-like, and triple-negative tumors had significantly higher pADC and p/tADC values than luminal A subtypes. These subtypes are known to exhibit more intense stromal remodeling and angiogenesis.^{36–39}

Notably, tADC did not differentiate tumor grade, whereas the p/tADC ratio did

($P = 0.004$ vs. $P = 0.252$). This supports the findings of Doğan et al.,⁴⁰ who argued that peritumoral diffusion metrics better reflect biological aggressiveness, and those of Choi et al.,⁴¹ who suggested that the p/tADC ratio mitigates variability introduced by tumor heterogeneity and imaging artifacts.

We also calculated cut-off values for predicting high-grade features. The optimal p/tADC threshold of 2.3, determined via ROC analysis, yielded the best balance between

sensitivity and specificity. The p/tADC ratio was moderately predictive across different features, with the highest LR+ for tumor size (LR+: 1.99) and the lowest for HER2 status (LR+: 1.56). Although not highly diagnostic on their own, these values offer quantifiable markers that can assist in clinical risk stratification.

In multivariate analysis, only high histological grade and Ki-67 $\geq 20\%$ retained statistical significance, emphasizing the p/tADC

ratio's closer relationship with proliferative activity and stromal remodeling rather than receptor expression per se.

Our findings are consistent with those of Okuma et al.,²⁸ who also identified associations between p/tADC and tumor size and grade, Ki-67, and lymph node status. Similarly, El-Metwally et al.⁴² supported a link between ADC metrics and Ki-67, whereas associations with hormone receptors were weaker.

Incorporating peritumoral diffusion metrics into breast MRI has been supported by a recent meta-analysis published in 2024 (PMID: 38334760).⁴³ However, many prior studies lacked interobserver reproducibility assessments or multivariate control. Our study addresses these gaps by demonstrating that the p/tADC ratio is not only reproducible (ICC > 0.90) but also an independent predictor of histopathological aggressiveness.

We also contributed to the literature by offering molecular subtype-specific analysis and defined p/tADC cut-offs for biologically aggressive features. Together, these findings position the p/tADC ratio as a promising adjunct to conventional MRI parameters for risk stratification in invasive breast cancer.

Our findings highlight the clinical value of the p/tADC ratio as a non-invasive imaging biomarker of tumor aggressiveness. The p/tADC ratio was independently associated with high histological grade and Ki-67 index and showed distinct patterns across molecular subtypes. By using a standardized ROI placement and defining specific cut-off values, this metric may aid in preoperative risk stratification. Integrating the p/tADC ratio into routine MRI protocols could support more personalized treatment planning. Future studies should also explore advanced diffusion techniques, such as diffusion tensor imaging, to better characterize peritumoral tissue heterogeneity.

Footnotes

Conflict of interest disclosure

The authors declared no conflicts of interest.

References

1. International Agency for Research on Cancer. Global Cancer Observatory: Cancer Today. Lyon, France: IARC; 2022. Accessed June 23, 2025. [\[Crossref\]](#)
2. Remšik J, Fedr R, Navrátil J, et al. Plasticity and intratumoural heterogeneity of cell surface antigen expression in breast cancer. *Br J Cancer*. 2018;118(6):813-819. [\[Crossref\]](#)
3. Zardavas D, Irtthum A, Swanton C, Piccart M. Clinical management of breast cancer heterogeneity. *Nat Rev Clin Oncol*. 2015;12(7):381-394. [\[Crossref\]](#)
4. Nelson DA, Tan TT, Rabson AB, Anderson D, Degenhardt K, White E. Hypoxia and defective apoptosis drive genomic instability and tumorigenesis. *Genes Dev*. 2004;18(17):2095-2107. [\[Crossref\]](#)
5. Polyak K, Kalluri R. The role of the microenvironment in mammary gland development and cancer. *Cold Spring Harb Perspect Biol*. 2010;2(11):a003244. [\[Crossref\]](#)
6. Hanahan D, Coussens LM. Accessories to the crime: functions of cells recruited to the tumor microenvironment. *Cancer Cell*. 2012;21(3):309-322. [\[Crossref\]](#)
7. Petitprez F, Meylan M, de Reyniès A, Sautès-Fridman C, Fridman WH. The Tumor microenvironment in the response to immune checkpoint blockade therapies. *Front Immunol*. 2020;11:784. [\[Crossref\]](#)
8. Hirata E, Sahai E. Tumor microenvironment and differential responses to therapy. *Cold Spring Harb Perspect Med*. 2017;7(7):a026781. [\[Crossref\]](#)
9. Beck AH, Sangoi AR, Leung S, et al. Systematic analysis of breast cancer morphology uncovers stromal features associated with survival. *Sci Transl Med*. 2011;3(108):108ra113. [\[Crossref\]](#)
10. Baltzer PA, Yang F, Dietzel M, et al. Sensitivity and specificity of unilateral edema on T2w-TSE sequences in MR-Mammography considering 974 histologically verified lesions. *Breast J*. 2010;16(3):233-239. [\[Crossref\]](#)
11. Cheon H, Kim HJ, Kim TH, et al. Invasive breast cancer: prognostic value of peritumoral edema identified at preoperative MR imaging. *Radiology*. 2018;287(1):68-75. [\[Crossref\]](#)
12. Kettunen T, Okuma H, Auvinen P, et al. Peritumoral ADC values in breast cancer: region of interest selection, associations with hyaluronan intensity, and prognostic significance. *Eur Radiol*. 2020;30(1):38-46. [\[Crossref\]](#)
13. Panzironi G, Moffa G, Galati F, Marzocca F, Rizzo V, Pediconi F. Peritumoral edema as a biomarker of the aggressiveness of breast cancer: results of a retrospective study on a 3 T scanner. *Breast Cancer Res Treat*. 2020;181(1):53-60. [\[Crossref\]](#)
14. Cvetković D, Cvetkovic A, Ninković S, Milutinovic M, Mitrović S, Marković S. The role of molecular markers of angiogenesis in disease prediction in breast cancer patients. *Biologia Serbica*. 2020;41(2):63-69. [\[Crossref\]](#)
15. Franchi M, Masola V, Bellin G, Onisto M, Karamanos KA, Piperigkou Z. Collagen fiber array of peritumoral stroma influences epithelial-to-mesenchymal transition and invasive potential of mammary cancer cells. *J Clin Med*. 2019;8(2):213. [\[Crossref\]](#)
16. Artacho-Cordón A, Artacho-Cordón F, Ríos-Arrabal S, Calvente I, Núñez MI. Tumor microenvironment and breast cancer progression: a complex scenario. *Cancer Biol Ther*. 2012;13(1):14-24. [\[Crossref\]](#)
17. Choyke PL, Dwyer AJ, Knopp MV. Functional tumor imaging with dynamic contrast-enhanced magnetic resonance imaging. *J Magn Reson Imaging*. 2003;17(5):509-520. [\[Crossref\]](#)
18. Bluemke DA, Gatsonis CA, Chen MH, et al. Magnetic resonance imaging of the breast prior to biopsy. *JAMA*. 2004;292(22):2735-2742. [\[Crossref\]](#)
19. Kul S, Cansu A, Alhan E, Dinc H, Gunes G, Reis A. Contribution of diffusion-weighted imaging to dynamic contrast-enhanced MRI in the characterization of breast tumors. *AJR Am J Roentgenol*. 2011;196(1):210-217. [\[Crossref\]](#)
20. Ginat DT, Mangla R, Yeane G, Johnson M, Ekholm S. Diffusion-weighted imaging for differentiating benign from malignant skull lesions and correlation with cell density. *AJR Am J Roentgenol*. 2012;198(6):W597-W601. [\[Crossref\]](#)
21. Anderson AW, Xie J, Pizzonia J, Bronen RA, Spencer DD, Gore JC. Effects of cell volume fraction changes on apparent diffusion in human cells. *Magn Reson Imaging*. 2000;18(6):689-695. [\[Crossref\]](#)
22. Hirano M, Satake H, Ishigaki S, Ikeda M, Kawai H, Naganawa S. Diffusion-weighted imaging of breast masses: comparison of diagnostic performance using various apparent diffusion coefficient parameters. *AJR Am J Roentgenol*. 2012;198(3):717-722. [\[Crossref\]](#)
23. Partridge SC, McDonald ES. Diffusion weighted magnetic resonance imaging of the breast: protocol optimization, interpretation, and clinical applications. *Magn Reson Imaging Clin N Am*. 2013;21(3):601-624. [\[Crossref\]](#)
24. Kim SH, Cha ES, Kim HS, et al. Diffusion-weighted imaging of breast cancer: correlation of the apparent diffusion coefficient value with prognostic factors. *J Magn Reson Imaging*. 2009;30(3):615-620. [\[Crossref\]](#)
25. Horvat JV, Bernard-Davila B, Helbich TH, et al. Diffusion-weighted imaging (DWI) with apparent diffusion coefficient (ADC) mapping as a quantitative imaging biomarker for prediction of immunohistochemical receptor status, proliferation rate, and molecular subtypes of breast cancer. *J Magn Reson Imaging*. 2019;50(3):836-846. [\[Crossref\]](#)
26. Uematsu T. Focal breast edema associated with malignancy on T2-weighted images of breast MRI: peritumoral edema, prepectoral edema, and subcutaneous edema. *Breast Cancer*. 2015;22(1):66-70. [\[Crossref\]](#)

27. Gemici AA, Ozal ST, Hocaoglu E, et al. Relation of peritumoral, prepectoral and diffuse edema with histopathologic findings of breast cancer in preoperative 3T magnetic resonance imaging. *J Surg Med.* 2019;3(1):49-53. [\[Crossref\]](#)
28. Okuma H, Sudah M, Kettunen T, et al. Peritumor to tumor apparent diffusion coefficient ratio is associated with biologically more aggressive breast cancer features and correlates with the prognostication tools. *PLoS One.* 2020;15(6):e0235278. [\[Crossref\]](#)
29. Woodhams R, Matsunaga K, Iwabuchi K, et al. Diffusion-weighted imaging of malignant breast tumors: the usefulness of apparent diffusion coefficient (ADC) value and ADC map for the detection of malignant breast tumors and evaluation of cancer extension. *J Comput Assist Tomogr.* 2005;29(5):644-649. [\[Crossref\]](#)
30. Hatakenaka M, Soeda H, Yabuuchi H, et al. Apparent diffusion coefficients of breast tumors: clinical application. *Magn Reson Med Sci.* 2008;7(1):23-29. [\[Crossref\]](#)
31. Quail DF, Joyce JA. Microenvironmental regulation of tumor progression and metastasis. *Nat Med.* 2013;19(11):1423-1437. [\[Crossref\]](#)
32. Junttila MR, de Sauvage FJ. Influence of tumour micro-environment heterogeneity on therapeutic response. *Nature.* 2013;501(7467):346-354. [\[Crossref\]](#)
33. Zhang H, Miao Q, Fu Y, et al. Intratumoral and peritumoral radiomics based on automated breast volume scanner for predicting human epidermal growth factor receptor 2 status. *Front Oncol.* 2025;15:1556317. [\[Crossref\]](#)
34. Harney AS, Arwert EN, Entenberg D, et al. Real-time imaging reveals local, transient vascular permeability, and tumor cell intravasation stimulated by TIE2hi macrophage-derived VEGFA. *Cancer Discov.* 2015;5(9):932-943. [\[Crossref\]](#)
35. Han Y, Huang M, Xie L, Cao Y, Dong Y. The value of intratumoral and peritumoral radiomics features based on multiparametric MRI for predicting molecular staging of breast cancer. *Front Oncol.* 2025;15:1379048. [\[Crossref\]](#)
36. Li X, Fang J, Wang F, Zhang L, Jiang X, Mao X. Prediction of HER2 expression in breast cancer patients based on multi-parametric MRI intratumoral and peritumoral radiomics features combined with clinical and imaging indicators. *Front Oncol.* 2025;15:1531553. [\[Crossref\]](#)
37. Fan M, He T, Zhang P, et al. Diffusion-weighted imaging features of breast tumours and the surrounding stroma reflect intrinsic heterogeneous characteristics of molecular subtypes in breast cancer. *NMR Biomed.* 2018;31(2). [\[Crossref\]](#)
38. Amini B, Ghasemi M, Rashidi F, et al. A comprehensive evaluation of quantitative diffusion parameters for differentiating histopathological features and subtypes of breast cancers: diffusion kurtosis imaging (DKI), intravoxel incoherent motion (IVIM) and histogram analysis of ADC. Preprint. Published January 3, 2023. [\[Crossref\]](#)
39. Zhao M, Fu K, Zhang L, et al. Intravoxel incoherent motion magnetic resonance imaging for breast cancer: a comparison with benign lesions and evaluation of heterogeneity in different tumor regions with prognostic factors and molecular classification. *Oncol Lett.* 2018;16(4):5100-5112. [\[Crossref\]](#)
40. Doğan GM, Siğirci A, Taşolar S, et al. Do intratumoral and peritumoral apparent diffusion coefficient (ADC) values have a role in the diagnosis of pediatric brain tumors? *Childs Nerv Syst.* 2020;36(3):251-259. [\[Crossref\]](#)
41. Choi EJ, Youk JH, Choi H, Song JS. Dynamic contrast-enhanced and diffusion-weighted MRI of invasive breast cancer for the prediction of sentinel lymph node status. *J Magn Reson Imaging.* 2020;51(2):615-626. [\[Crossref\]](#)
42. El-Metwally D, Monier D, Hassan A, Helal AM. Preoperative prediction of Ki-67 status in invasive breast carcinoma using dynamic contrast-enhanced MRI, diffusion-weighted imaging and diffusion tensor imaging. *Egypt J Radiol Nucl Med.* 2023;54(1):62. [\[Crossref\]](#)
43. Zhao S, Li Y, Ning N, et al. Association of peritumoral region features assessed on breast MRI and prognosis of breast cancer: systematic review and meta-analysis. *Eur Radiol.* 2024;34(9):6108-6120. [\[Crossref\]](#)